Cycling behaviour of electrodeposited zinc alloy electrode for secondary lithium batteries

Takuya Fujieda, Sachio Takahashi and Shunichi Higuchi

Government Industrial Research Institute, Osaka 1-8-31 Midorigaoka, Ikeda, Osaka (Japan)

Abstract

The cycling behaviour of an electroplated lithium–zinc alloy film electrode is examined in 1 M LiClO$_4$/propylene carbonate. The cycle life depends on the utilization of lithium in the alloy and is improved by dispersion of 2 to 4 wt.% iron. This improvement is more effective when the discharge cutoff potential is 0.5 V versus Li$^+$/Li. In this case, the life cycle is about 150 cycles at 250 mA h g^{-1} of lithium utilization. The reason for improvement is possibly the suppression of electrode disintegration and the appropriate choice of alloy phases.

Introduction

Since Dey [1] reported that electrodeposited lithium can easily alloy with foreign substrates, many attempts have been made to use it as practical anodes for secondary lithium batteries [2]. The most outstanding advantage of alloy anodes is high rate of utilization of Li for charge/discharge cycling [3]. If pure Li metal is used as an anode in LiClO$_4$/propylene carbonate (PC), the efficiency losses of Li are close to 20% [4]. Several alloy electrodes, however, show only a few percent loss for each cycle. Cycling efficiency is the criterion not only for energy efficiency but also for cycle life [5]. Thus, high cycling efficiency should lead to long cycle life. Alloy electrodes collapse via microcracks and pulverization owing to the occurrence of large volume differences between the phases in the alloy during cycling [6].

To solve this lithium-performance problem, an attempt has been made to find additives and alloy phases with excellent life cycle. Lithium alloying elements form fragile intermetallic compounds and disintegrate mechanically. Thus, elements that do not react with Li are considered to be promising as additives to Li alloying metals. To this end, an investigation has been made of Cu, Ni, Co and Fe additives to a Zn substrate. Significant effects have been found in the case of Fe. In this paper, the cycling behaviour of electroplated Li–Zn and Li–Zn–Fe alloy film electrodes is reported.

Experimental

All electrodes were prepared by the electrodeposition of Zn or Zn–Fe alloy on Ni wire (1 mm diameter × 1 cm = 0.32 cm^2) in sulfate baths. The Fe content in the deposits was varied by changing the composition of the bath (i.e. 1.5 to 2.0 M ZnSO$_4$, 0 to 0.7 M FeSO$_4$) and current density (15 to 60 mA cm^{-2}). Electrodeposition was

followed by heat treatment (200 to 250 °C) under nitrogen for 15 min. Ten electrodes were made under the same conditions, and three of each were dissolved in HCl for quantitative analysis of Zn and Fe by atomic absorption spectrophotometry. The average content was considered to be the same as that of the seven other electrodes that were used for cycling tests.

Cycling tests were conducted in 1 M $LiClO_4$/PC (~ 50 ml) using conventional three-electrode cells with a potentiogalvanostat (Hokuto Denko, HA501G) controlled by a personal computer. The counter and reference electrodes were Li ribbons of ~ 4 cm^2 area. All potentials were recorded versus Li^+/Li. Charging and discharging were carried out at 0.33 mA cm^{-2}. Charging was terminated by time, discharge by potential. Cycling efficiency was determined by dividing the discharge time by the charge time. The purity of the individual chemicals was: $ZnSO_4 \cdot 7H_2O(99.9\%)$, $FeSO_4 \cdot 7H_2O(99.5\%)$, $LiClO_4$ (99%), Li(99.8%), and PC(99%). The $LiClO_4$ was vacuum-dried at 150 °C for more than 3 days and dissolved in distilled PC just before use. Storage and handling were performed in a dry box with a purified argon atmosphere.

Results and discussion

The effects of thickness of the plated Zn electrode on cycle life were examined in 1 M $LiClO_4$/PC. This study was carried out to clarify the determining factors of cycle life. Basically, this experiment was to investigate the influence on cycle life of (i) chemical reactions at the surface of the Zn electrode and (ii) the utilization of Li in the anode. Electrodes with three different thicknesses were prepared and tested. The life cycle was defined as that having an efficiency of $>90\%$. Because the potential at rest after charging was significantly higher than the equilibrium potential of Li/ Li^+, the efficiency was $>90\%$. The results are shown in Table 1. The electricity passing through the surface of the electrode is proportional to the thickness of the Zn layer

TABLE 1

Cycle life of electroplated zinc electrodes with three different thicknesses and three utilizations of lithium

	Thickness (μm)	Utilization		
		250 mA h g^{-1}	167 mA h g^{-1}	83 mA h g^{-1}
1	0.42	35 38	129 142 132	318
2	0.85	37 37 45	112 124	333 324
3	1.70	54 45	107 95	308 329 349

Charge/discharge current density: 0.33 mA cm^{-2}. Rest time after charge or discharge: 30 min. Charge time: (1) 15, 10, 5 min; (2) 30, 20, 10 min; (3) 60, 40, 20 for lithium utilizations of 250 to 83 mA h g^{-1}, respectively. Discharge cutoff potential: 1.0 V vs. Li^+/Li.

if compared for the same utilization of Li. Clearly, the cycle life exhibits little dependence on the thickness of the Zn layer but is effected appreciably by the utilization of Li in the Zn anode. Even at a utilization of 250 mA h g^{-1} (charge capacity/Zn weight), all the deposited Li was alloyed during 30 min. The composition of the anode during cycling can be expressed as follows:

$$Li_{x+\Delta Y}Zn \qquad 0 \leq \Delta Y \leq Y \qquad (1)$$

where X is the retention of Li at discharge and ΔY is the charge/discharged Li per unit Zn and related to the utilization of Li in the alloy. At 250 mA h g^{-1}, $Y = 0.6$. This is suitable for practical application in secondary batteries with respect to energy density. At this value, however, cycle life was <50 as shown in Table 1. At low utilization, the performance improved and the total discharge capacity throughout life also became larger.

Scanning electron micrographs of the electrode after the Li cycling test at 250 mA h g^{-1} are presented in Fig. 1. The hexagonal crystals prior to cycling disappeared and small particles developed after the cycle test. The particle contact appeared inadequate. In fact, precipitates from the surface of the electrode were often observed at the bottom of the cell at the end of the cycle test. The main reason for degradation of the Zn electrode was considered to be a morphological change to fine particles that were probably not in contact with each other.

To improve cycle life, Fe, Co, Ni, and Cu were added to the Zn by alloy electrodeposition. Among these, the Fe–Zn alloy anode displayed significantly longer life cycle that the pure Zn counterpart. Figure 2 shows the cycling efficiency of the pure Zn and Zn–Fe alloy electrodes against cycle number for a Li utilization of 250 mA h g^{-1}. The addition of 2 to 4 wt.% Fe improved the performance by 20 to 30 cycles. When the Fe content exceeded 4 wt.%, however, the cycle life became shorter, although the initial cycling efficiency was better. The difference in cycle life between electrodes with and without Fe became greater when the discharge cutoff potential was lowered to 0.5 from 1.0 V. This effect will be discussed later.

The electrodeposited Zn–Fe binary alloy forms a supersaturated solid solution (η-phase) in the zinc-rich region [7]. At equilibrium, the solubility of Fe in Zn is
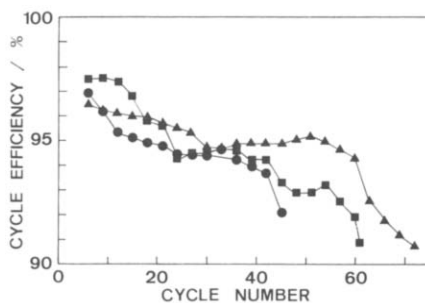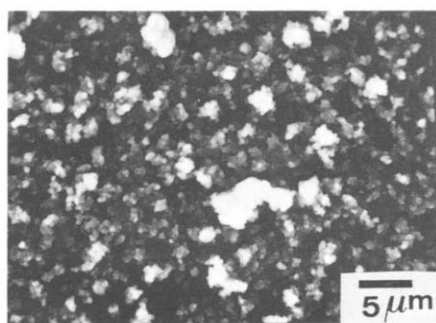

Fig. 1. Scanning electron micrograph of electroplated zinc electrodes after 49 cycles in discharged state. Charge/discharge current density: 0.33 mA cm^{-2}; charge time and rest time after charge or discharge: 30 min; lithium utilization: 250 mA h g^{-1}; discharge cutoff potential: 1.0 V.

Fig. 2. Cycling efficiency (discharge time × 100/charge time) for (●): zinc, (▲): zinc–2wt.% iron and (■): zinc–5wt.% iron anode at 250 mA h g^{-1} as function of cycle number. Cycling conditions same as in Fig. 1.

0.02 wt.% [8], but more than 3 wt.% in the electrodeposited alloy. This was confirmed by a continuous change in the lattice constants, namely, increase in the a-axis and decrease in the c-axis. The supersaturated solid solution was stable at room temperature but relaxed to an equilibrium η-phase having almost the same lattice constants as pure zinc near 200 °C. Even in the case of a Zn–Fe substrate before heat treatment, electrodeposited Li alloyed with the substrate. This indicates that *meta*-stable η-phase formation does not inhibit the reaction between Li and Zn. The features of the discharge curves of Zn–Li and Zn–Fe–Li were essentially the same, each showed three plateaus, although polarization of the latter was significant. Heat treatment of Zn–Fe (<4 wt.% Fe) electrodes increases the initial cycling efficiency and cycle life. On the other hand, for Fe contents >4 wt.%, heat treatment decreased cycle life.

The morphology of the surface of the Zn–Fe electrode after the Li cycling test is given in Fig. 3. The morphological change observed for the Zn electrode (Fig. 1) is not discernible. The surface regions are relatively compact and in close contact with each other. The introduction of Fe suppresses pulverization of the electrode and this is probably the main reason for the longer life. For the electrode containing >4 wt.% Fe, favourable effects on cycle life were not found. Collapse of the electrode as noted for pure Zn was observed. X-ray diffraction profiles of Zn–Fe substrates containing >4 wt.% Fe showed unidentified peaks that were absent in alloys having less than 4 wt.% Fe. Contamination of Zn–Fe intermetallic compounds (possibly distorted Γ-phase) may thus destabilize the electrode morphology during Li deposition-dissolution cycling.

Figure 4 shows charge/discharge curves for the Zn–Fe–Li electrode at the initial, middle and end stages of cycle life. During the first few cycles, the potential during charge was lower than the equilibrium potential of Li. It became positive after about 10 cycles, and this suggests that the Li alloying rate was now faster than the Li deposition rate. The potential during rest after charging was positive throughout the cycle life. The most important point to be noted is the change in the discharge curve with cycle life. Initially, the main discharge potential was at a plateau of 240 to 270 mV versus Li/Li$^+$. The surface may have consisted of LiZn and Li$_2$Zn$_3$ given the reported equilibrium potentials of the alloys [9]. But discharge from this plateau was replaced by that from higher potentials with increase in cycle number. This would
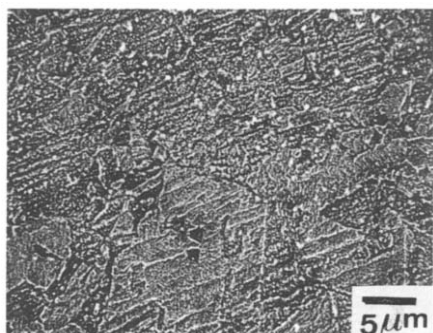

Fig. 3. Scanning electron micrograph of electroplated zinc–iron electrode after 77 cycles in discharged state. Cycling conditions same as in Fig. 1.
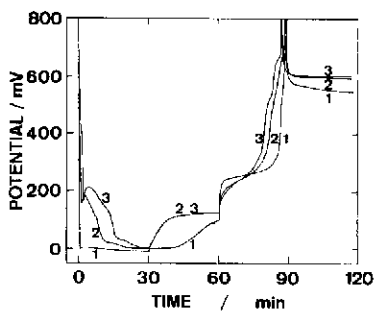
Fig. 4. Charge/discharge curves with electroplated zinc–iron electrode at (1) 5, (2) 25, (3) 60 cycles for discharge cutoff of 1.0 V vs. Li$^+$/Li. Cycling conditions same as in Fig. 1.

suggest the accumulation of alloys such as $LiZn_2$ and Li_2Zn_5 with a greater positive equilibrium potential. The changes in alloy phases were considered to be responsible for the degradation of the Zn–Fe alloy electrode. Therefore, the relationship between the alloy phase at discharge and cycle life was studied.

The influence of cutoff potential on life cycle was examined. The phases that appeared during discharge could be controlled by varying the cutoff voltage of discharge. In this experiment, X in eqn. (1) was varied by changing the discharge cutoff potential and ΔY was fixed at 250 mA h g^{-1}. Typical cycling efficiency values at each cycle are plotted in Fig. 5 for three cutoff potentials. The cyclic voltammogram for the Zn electrode in 1 M $LiClO_4$/PC showed 4 peaks in Fig. 6. These were identified from the equilibrium potential of each phase. At potentials of 1.0 and 2.0 V versus Li^+/Li, the discharge was cut off during discharge from Li_2Zn_5 phase. The diffusion of Li in Li_2Zn_5 is very slow [9] compared with that in the other three phases and thus the potential increases from 1.0 to 2.0 V very rapidly (for ~10 s) at the end of discharge. Accordingly, the difference in X is only slight at cutoff potentials of 1.0 and 2.0 V. There was, however, a considerable difference in cycle life, as shown in Fig. 5. The life cycle cutoff at a potential of 2.0 V was half that at 1.0 V. When the discharge was cut off at 0.5 V, the life cycle became twice that at 1.0 V. In this case, Li_2Zn_5 may not have formed on the surface. Discharge from Li_2Zn_5 would thus appear disadvantageous for increasing cycle life. Indeed, elimination of the discharge from Li_2Zn_5 improved cycle life greatly.

A low discharge cutoff potential showed no effects for a Zn (not containing Fe) electrode. The cycle life was 50 to 60 cycles even when discharge was cut off at 0.5 V. This performance is slightly better than that at 1.0 V (35 to 50 cycles, see Table 1). The cause of the degradation of the Li–Zn electrode was considered to be the morphological change shown in Fig. 1, for the situation where the discharge was cut off at 0.5 V. Control of alloy phase may thus be an effective approach to increasing cycle life only when there are no morphological problems. The charge/discharge curves
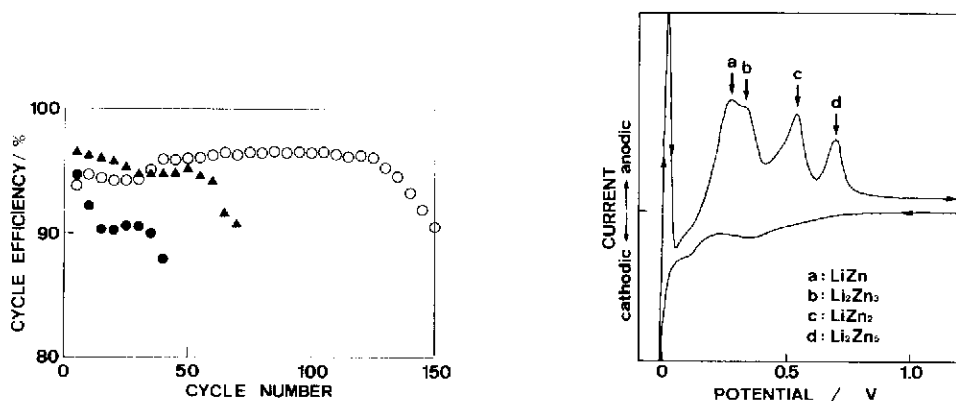

Fig. 5. Cycling efficiency (discharge time × 100/charge time) of zinc–iron electrode at 250 mA h g^{-1} vs. cycle number at discharge cutoff potential: (●) 2.0 V, (▲) 1.0 V, (○) 0.5 V vs. Li^+/Li. Charge/discharge current density: 0.33 mA cm^{-2}, charge time, rest time after charge and discharge: 30 min.

Fig. 6. Cyclic voltammogram for zinc in 1 M $LiClO_4$ in propylene carbonate. Reversal potentials: −0.03 V and 2.0 V vs. Li^+/Li; sweep rate: 4 mV s^{-1}.
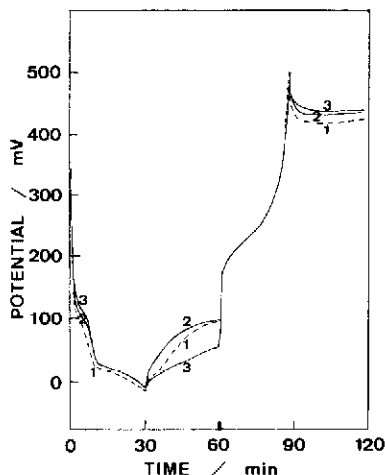
Fig. 7. Charge/discharge curves of electroplated zinc–iron electrode at (1) 25, (2) 50, (3) 100 cycles for discharge cutoff of 0.5 V vs. Li^+/Li. Charge/discharge current density: 0.33 mA cm^{-2}; rest after charge or discharge: 30 min, at 250 mA h g^{-1} of lithium utilization.

for a cutoff potential of 0.5 V changed with cycling, as shown in Fig. 7. In contrast to the data shown in Fig. 3, the discharge curves did not change throughout cycle life. Under these conditions, accumulation of low Li content Li–Zn alloys was not observed. This may be related to the remarkable improvement in cycle life when lowering the cutoff potential. The slow diffusion of Li in Li_2Zn_5 is not the reason for the accumulation of the zinc-rich phase. This is because the charge/discharge characteristics show that the kinetics of transformation from/to Li_2Zn_5 to/from other phases are sufficiently fast for the electrode to act as a reversible system. Rather, the irreversibility may be related to irreversible chemical reactions between the alloy and electrolyte solution at locally generated Li_2Zn_5 at the end of discharge. Consequently, control of alloy phases is important for a multiphase Li alloy electrode.

Conclusions

The cycle life of an electrodeposited Zn electrode is improved by dispersion of 2 wt.% Fe. The effect is greater when the discharge cutoff potential is 0.5 V versus Li^+/Li. In this case, the cycle life is about 150 cycles at 250 mA h g^{-1}.

Two factors that determine the cycle life of the alloy electrode have been clarified, namely, collapse of an alloy and, possibly, irreversible chemical reactions occurring with the discharge, especially from Li_2Zn_5. The former problem is ameliorated by the addition of Fe to the alloy, the latter problem by lowering the discharge cutoff potential.

References

1 A. N. Dey, *J. Electrochem. Soc.*, *118* (1971) 1547.
2 J. R. van Beek and P. J. Rommers, in J. Thompson (ed.), *J. Power Sources*, Academic Press, London, 1979, p. 595; R. A. Huggins, *J. Power Sources*, *26* (1989) 109.

3 A. S. Baranski, W. R. Fawsett, T. Krogulec and M. Drogowska, *J. Electrochem. Soc., 131* (1984) 1750.
4 S. Tobishima, J. Yamaki, A. Yamaji and T. Okada, *J. Power Sources, 13* (1984) 261.
5 R. Selim and P. Bro, *J. Electrochem. Soc., 121* (1974) 1457.
6 Y. Geronov, P. Zlatilova and R. V. Moshtev, *J. Power Sources, 12* (1984) 145; W. C. Maskell and J. R. Owen, *J. Electrochem. Soc., 132* (1985) 1602.
7 K. Kondo, S. Hinotani and Y. Ohmori, *J. Appl. Electrochem., 18* (1988) 154.
8 M. Hansen and K. Anderko (eds.), *Constitution of Binary Alloys,* 2nd ed., McGraw-Hill, New York, 1986, p. 737.
9 J. Wang, P. King and R. A. Huggins, *Solid State Ionics, 20* (1986) 185.